JVI Journals.ASM.org

Acid-Activated Structural Reorganization of the Rift Valley Fever Virus Gc Fusion Protein

S. M. de Boer,[a,b] J. Kortekaas,[b] L. Spel,[a] P. J. M. Rottier,[a] R. J. M. Moormann,[a,b] and B. J. Bosch[a]

Department of Infectious Diseases and Immunology, Virology Division, Faculty of Veterinary Medicine, Utrecht University, Utrecht, The Netherlands,[a] and Central Veterinary Institute of Wageningen University and Research Centre, Department of Virology, Lelystad, The Netherlands[b]

The entry of the enveloped Rift Valley fever virus (RVFV) into its host cell is mediated by the viral glycoproteins Gn and Gc. We investigated the RVFV entry process and, in particular, its pH-dependent activation mechanism using our recently developed nonspreading-RVFV-particle system. Entry of the virus into the host cell was efficiently inhibited by lysosomotropic agents that prevent endosomal acidification and by compounds that interfere with dynamin- and clathrin-dependent endocytosis. Exposure of plasma membrane-bound virions to an acidic pH (<pH 6) equivalent to the pH of late endolysosomal compartments allowed the virus to bypass the endosomal route of infection. Acid exposure of virions in the absence of target membranes triggered the class II-like Gc fusion protein to form extremely stable oligomers that were resistant to SDS and temperature dissociation and concomitantly compromised virus infectivity. By targeted mutagenesis of conserved histidines in Gn and Gc, we demonstrated that mutation of a single histidine (H857) in Gc completely abrogated virus entry, as well as acid-induced Gc oligomerization. In conclusion, our data suggest that after endocytic uptake, RVFV traffics to the acidic late endolysosomal compartments, where histidine protonation drives the reorganization of the Gc fusion protein that leads to membrane fusion.

Rift Valley fever virus (RVFV) is an emerging pathogen that affects ruminants and humans and is transmitted between susceptible hosts by different species of mosquitoes. RVFV was first isolated in Kenya in 1930 and has since spread throughout the African continent and the Arabian Peninsula (12, 46). An outbreak of RVFV can have a devastating socioeconomic impact on the region (2, 18, 50) and is characterized by abortion storms in adult livestock and high mortality among newborns. Humans can also be infected through contact with infected tissues or via mosquito bites, typically causing a self-limiting febrile illness. A small percentage of human infections result in hemorrhagic fever or encephalitis with generally fatal outcome (41).

RVFV belongs to the *Phlebovirus* genus of the *Bunyaviridae* family, which comprises four additional genera (*Orthobunyavirus*, *Hantavirus*, *Nairovirus*, and *Tospovirus*). Members of the *Bunyaviridae* family are enveloped viruses of ~100 nm in size that have a tripartite negative-strand RNA genome which is replicated in the cytoplasm. The genomic segments are encapsidated by the nucleocapsid protein, forming the ribonucleoproteins (RNPs) (56). The lipid envelope surrounding the RNPs contains an ordered shell made up by units of two glycoproteins, Gn and Gc (20). These glycoproteins are responsible for entry into the host cell, but their precise functional roles in receptor binding and fusion are poorly understood. Gn and Gc are type I membrane glycoproteins which form heterodimers after posttranslational processing of a glycoprotein precursor in the endoplasmic reticulum. By virtue of a Golgi localization signal in Gn, the Gn-Gc heterodimers are targeted to the Golgi apparatus (56, 65). Here, interaction between the Gn carboxyl-terminal cytoplasmic tail and the RNPs allows virus budding into the lumen of the Golgi cisternae (45, 47, 56). In the case of the RVFV virion, a 78-kDa protein consisting of pre-Gn and Gn regions has been identified as a third but minor structural component (27, 60). Cryoelectron microscopy studies of RVFV virions showed that the viral envelope comprises 720 heterodimers of Gn (54 kDa) and Gc (56 kDa), forming 110 cylinder-shaped hexamers and 12 pentamers according to a T=12 icosahedral lattice (13, 24).

Enveloped viruses carry dedicated proteins in their envelope which mediate fusion between viral and cellular membranes, allowing translocation of the viral genome into the cytoplasm. This membrane fusion process is driven by structural rearrangements in the metastable viral fusion protein which are triggered by receptor binding, proteolytic cleavage, or the acidic pH of endosomes, allowing fusion to occur at the right time and place (8). Viral fusion proteins have been divided into three classes (classes I, II, and III) based on their structural features (67). The Gc glycoprotein of bunyaviruses has been proposed to be a class II viral fusion protein (15, 53). Similar to class II fusion proteins of alphaviruses and flaviviruses, Gc is predicted to be mainly composed of β-sheet structures, is synthesized from a polyprotein downstream of a companion protein (Gn), and assembles into a heterodimer in the ER (15, 48, 62, 63).

Common to all class II fusion proteins is that they utilize the low pH in the acidified endosome to activate their fusion process. Low pH triggers the dissociation of the glycoprotein dimeric state, resulting in the exposure and subsequent insertion of a highly hydrophobic stretch of amino acids. Insertion of this fusion peptide into the target membrane is followed by trimerization of the monomeric fusion proteins. A stable trimeric hairpin structure is subsequently formed which brings together the fusion peptide and transmembrane domain at one end of the molecule, mediating the fusion of the cellular and viral membrane. While the acid-induced conformational changes of class II viral fusion proteins

Received 29 July 2012 **Accepted** 28 September 2012
Published ahead of print 3 October 2012
Address correspondence to B. J. Bosch, b.j.bosch@uu.nl.

doi:10.1128/JVI.01973-12

have been well documented (for an comprehensive review, see reference 30), the mechanism of low-pH triggering is not well understood. Protonation of histidines has been suggested to act as a molecular switch that triggers the activity of pH-activated viral fusion proteins (4, 28). The rationale for this hypothesis is that histidine is the only amino acid residue with a side chain pK_a value (pK_a 6.4) within the pH range found in the endolysosomal pathway (pH 4.5 to 6.5) (28, 54). Evidence in support of a crucial role for histidine protonation in promoting fusion protein rearrangements leading to fusion has been obtained for a number of low-pH-dependent viruses (3, 4, 6, 14, 26, 34, 36, 49, 57, 61).

Knowledge of the fusion mechanism of bunyaviruses is still in its infancy. In agreement with a class II virus classification, bunyaviruses appear to have an acid-dependent fusion machinery. Exposure of cells overexpressing RVFV Gn and Gc to low pH results in the formation of multinucleated cells (11). Acid-induced syncytium formation has also been reported for other members of the *Bunyaviridae* family, including Uukuniemi virus (UUKV, *Phlebovirus* genus), La Crosse virus (*Orthobunyavirus* genus), and Hantaan virus (*Hantavirus* genus) (1, 39, 42, 48). In accordance with the hypothesis of acid-induced fusion activation, bunyaviruses are sensitive to acidotropic agents which raise the pH of intracellular endocytic compartments (55, 58). In addition, acid exposure of plasma membrane-bound UUKV could bypass the endosomal acidic pH requirement needed for infection (39).

In this study, we have examined the entry mechanism of RVFV. Studies of natural RVFV strains have been hampered by the requirement of handling the virus under biosafety level 3 (BSL3) containment. We have taken advantage of our recently established nonspreading-RVFV ($RVFV_{ns}$) production system, which can be handled outside BSL3 containment (33). This system allows the efficient production of RVFV particles upon transfection of a single Gn/Gc expression plasmid into a replicon cell line which maintains the replication machinery of RVFV. The expression of the enhanced green fluorescent protein (eGFP) gene from the viral genome enables infection to be easily monitored. Most importantly, the system greatly facilitates Gn and Gc structure/function studies as long as particle assembly is not compromised. Using $RVFV_{ns}$, we have examined the endocytic uptake of the virus, the low-pH dependence and kinetics of virus entry, and the effects of low-pH treatment of the virus on infectivity and rearrangement of the glycoproteins, as well as the role of conserved histidines in Gn and Gc in virus entry.

MATERIALS AND METHODS

Cells and viruses. BHK cells were grown in Glasgow minimum essential medium (GMEM; Invitrogen) supplemented with 4% tryptose phosphate broth, 1% minimum essential medium nonessential amino acids (MEM NEAA; Invitrogen), and 5% (vol/vol) fetal calf serum (FCS; Bodinco). For maintenance of BHK-Rep2 cells (33), geneticin (G-418) was used at a concentration of 1 mg/ml. A549 and CHO K1 cells were grown in Dulbecco's modified Eagle's medium (DMEM; Lonza Biowhittaker) and Ham's F-12K medium (Invitrogen), respectively, supplemented with 10% FCS. Cells were grown at 37°C and 5% CO_2. *Drosophila* Schneider (S2) cells (Invitrogen) were grown at 27°C in serum-free InsectXpress medium (Lonza). Recombinant RVFV ($RVFV_{rec}$) and $RVFV_{ns}$ have both been rescued from cDNA as described previously (33). VSV-ΔG/GFP/G* is a recombinant vesicular stomatitis virus (VSV) whose glycoprotein gene has been replaced by the GFP gene. The virus was pseudotyped with its authentic glycoprotein G as described previously (5).

Plasmids. The QuikChange XL site-directed mutagenesis kit (Stratagene) was used according to the manufacturer's protocol to exchange specific histidine for alanine codons in the pCAGGS-M expression plasmid (33) at amino acid positions 157, 540, 572, 580, 778, 836, 857, and 1087 of the RVFV M segment (GenBank sequence accession number JF784387). The recombinant plasmids were sequenced to confirm that only the desired mutations were present.

To generate a stable *Drosophila* S2 cell line expressing the Gc ectodomain (Gce) of RVFV (GenBank sequence accession number JF784387), a truncated version of the Gn-Gc coding sequence lacking the transmembrane and cytoplasmic domains of Gc (GnGce; 153-AEDPHL/FGGPLK-1158) was cloned into the pMT/BiP/V5-HisA (Invitrogen) expression vector downstream from the BiP-encoding signal sequence. A quadruple Strep tag-encoding sequence separated by glycine linkers [DPTGWSHP QFEK(GGGSGGGSGGGSWSHPQFEK)^3] was appended C terminally to allow purification of the secreted Gc ectodomain from the culture supernatant using Strep-Tactin Sepharose affinity chromatography (IBA GmbH). Stable S2 cell lines were generated according to the manufacturer's protocol (Invitrogen) with minor modifications. S2 cells were transfected with the expression vector and pCoBlast plasmid in a 1:19 ratio. Stable cell lines were subsequently selected at 27°C in serum-free InsectXpress medium containing 25 μg/ml blasticidin-S-HCl (Invitrogen) and maintained in this culture medium in the presence of 10 μg/ml blasticidin-S-HCl.

Production of polyclonal antiserum against Gc ectodomain. Polyclonal antibodies were raised against the Gc ectodomain after immunization of rabbits (Davids Biotechnologie). Rabbits were immunized at days 0, 14, and 21 with ~40 μg of Strep tag-purified Gc ectodomain. Total serum was collected at day 35.

Chemicals. Bafilomycin A1, dynasore, cytochalasin D, nystatin (Sigma), and dyngo-4a (Abcam) were prepared in dimethyl sulfoxide (DMSO). Chlorpromazine and ammonium chloride (Sigma) were prepared in distilled sterile water. Diethyl pyrocarbonate (DEPC; Sigma) was dissolved in 96% ethanol.

Fluorescence-activated cell sorting (FACS). Flow cytometry was performed on a FACSCalibur flow cytometer (Becton, Dickinson Immunocytometry Systems). For the analysis of the data, Cyflogic 1.2.1 software was used.

Fluorescence microscopy. Fluorescence microscopy on living or fixed cells (fixed with 3.7% formaldehyde for 20 min at room temperature) was performed on the EVOS fl microscope (AMG). Nuclei of fixated cells were stained with 4′-6-diamidino-2-phenylindole (DAPI).

Production of $RVFV_{ns}$ particles. $RVFV_{ns}$ particles were produced as described previously (33). In short, BHK-rep2 cells (33) were seeded in Opti-Mem medium (Invitrogen) supplemented with 2% FCS. Cells were transfected (JetPEI; Polyplus) with pCAGGS-M (or derivatives thereof) in Opti-Mem containing 0.2% FCS. Twenty hours posttransfection, the $RVFV_{ns}$ particles in the collected medium were concentrated and transferred into a phosphate-buffered saline (PBS) or HNE (5 mM HEPES, 150 mM NaCl, 0.1 mM EDTA) buffer, pH 7.4, using Amicon Ultra centrifugal filters (Millipore) with a molecular mass cutoff of 100,000 kDa (Millipore). Titers of $RVFV_{ns}$ stocks were determined by 50% tissue culture infective dose ($TCID_{50}$) analysis as described previously (33).

Inhibition of RVFV infection by pharmacological drugs. To analyze the effects of specific drugs on RVFV entry, BHK-21 cells were pretreated for 1 h with ammonium chloride, chlorpromazine (both dissolved in water), bafilomycin A1, cytochalasin D, dynasore, dyngo-4a, or nystatin (the latter five dissolved in DMSO). Cells were inoculated for 2 h with $RVFV_{ns}$ or VSV_{ns} (VSVΔG-GFP/G*) (multiplicity of infection [MOI] of ~0.4) at 37°C before the culture medium was replaced with medium containing 10 or 40 nM bafilomycin A1, respectively. Cells were further incubated at 37°C. The inhibitory effects of the compounds on virus replication were tested by the addition of the chemicals 2 h postinfection (h.p.i.). After a period of 3 h, the drug-containing medium was replaced with culture medium containing bafilomycin (10 nM). $RVFV_{ns}$ or VSV_{ns} infection was

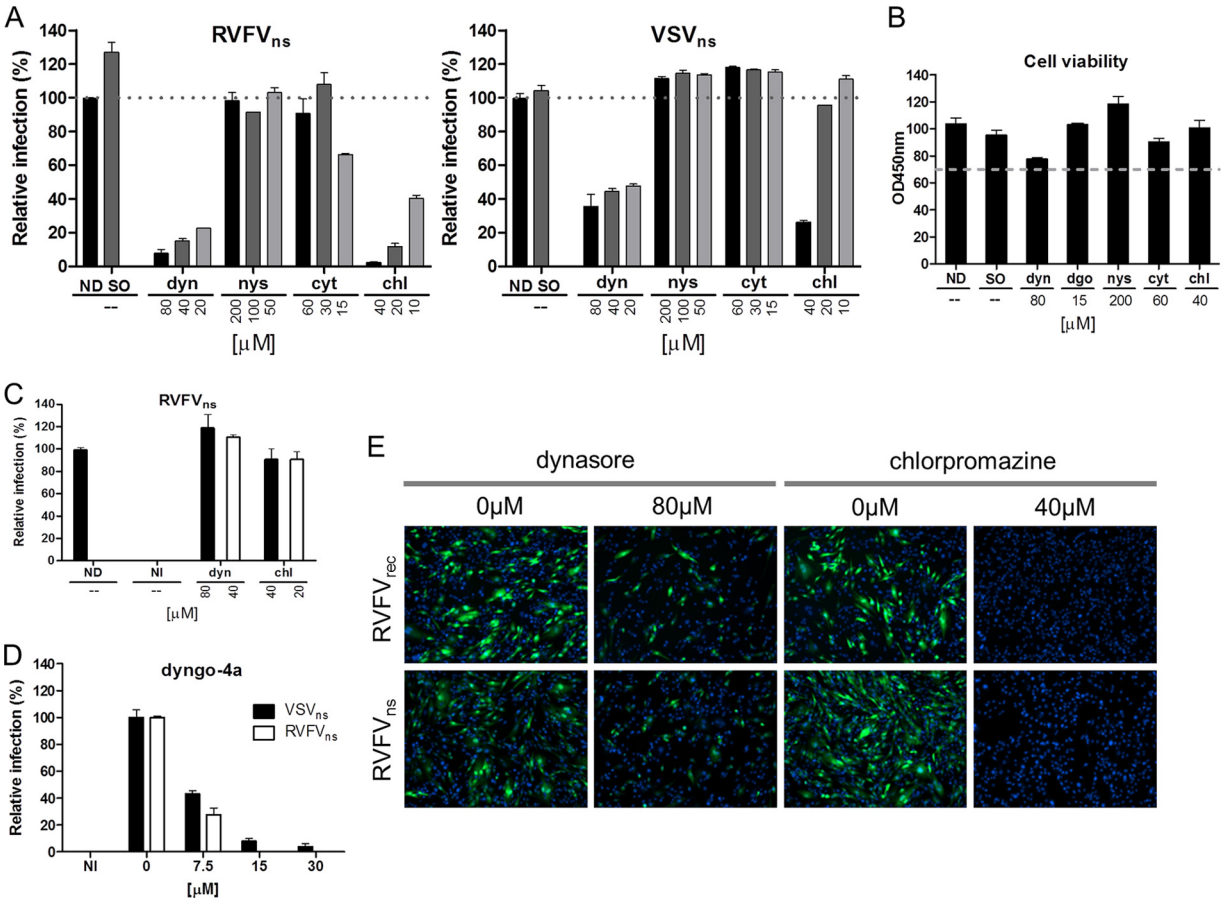

FIG 1 Rift Valley fever virus enters the cell via endocytosis. (A) BHK-21 cells were pretreated for 1 h with 2-fold dilutions of the indicated drugs and inoculated with RVFV$_{ns}$ (MOI of ~0.1) or VSV$_{ns}$ (MOI of ~0.8) for 2 h in the continued presence of the drugs, after which the inoculum was replaced by culture medium containing bafilomycin A1 (10 to 40 nM) to inhibit further RVFV entry (see Fig. 2). Infection was quantified 20 h (RVFV$_{ns}$) or 8 h (VSV$_{ns}$) postinfection by measuring GFP-positive cells using FACS. The data are the means of three independent experiments done in duplicate. ND, no drugs; SO, solvent (1% DMSO); dyn, dynasore; nys, nystatin; cyt, cytochalasin D; chl, chlorpromazine. (B) BHK-21 cells were incubated with the indicated drugs for 3 h, after which medium containing the drugs was replaced with culture medium containing bafilomycin A1 (20 nM). Twenty hours later, the effect of the chemical compounds on the metabolic activity of the cells was determined using a spectrophotometric assay. Cells were considered viable if the metabolic activity of treated cells remained above 70% (indicated by the dashed line) relative to that of untreated cells (ND). The results shown are representative of two independent experiments performed in triplicate. OD_{450}, optical density at 450 nm; dgo, dyngo-4a. (C) BHK-21 cells were infected with RVFV$_{ns}$ (MOI of ~0.2) for 2 h, after which infection was continued for 3 h in the presence of 80 or 40 μM dynasore or 20 or 40 μM chlorpromazine. Cells were incubated overnight in culture medium containing bafilomycin A1 (20 nM). At 20 h postinfection, infected (GFP-positive) cells were quantified by FACS. Data shown are representative of two independent experiments performed in duplicate. NI, not infected. (D) Analysis of the effect of dyngo-4a on RVFV$_{ns}$ and VSV$_{ns}$ infection (MOI of ~0.4) of BHK-21 cells. Infection was performed and quantified as described for panel A. (E) Representative fluorescence pictures of BHK-21 cells infected with RVFV$_{ns}$ or RVFV$_{rec}$ in the presence of dynasore (80 μM) or chlorpromazine (40 μM). Infection was performed as described for panel A at an MOI of ~0.2. Nuclei were stained with DAPI. Pictures are representative of two independent experiments performed in duplicate.

quantified at 20 or 8 h after virus inoculation, respectively, by analysis of GFP-expressing cells using FACS or fluorescence microscopy. The viability of the drug-treated cells was measured using a WST-1 assay (Roche) according to the manufacturer's recommendations.

Ammonium chloride add-in time course. Infection was synchronized by allowing RVFV$_{ns}$ particles to bind to cells on ice for 1 h in serum-free medium. The cells were washed with cold medium to remove unbound virus and subsequently transferred rapidly to a 37°C water bath after the addition of serum-free prewarmed Roswell Park Memorial Institute 1640 medium (RPMI 1640; Invitrogen) adjusted at different pHs. Ammonium chloride (10 mM) was added to the medium at the indicated times. Infection (GFP-positive cells) was quantified by FACS and fluorescence microscopy at 18 h after warming.

Polyacrylamide gel electrophoresis, Western blotting, and dot blot analysis. Samples containing RVFV$_{ns}$ particles were heated for 10 min at 40 to 80°C in Laemmli sample buffer lacking β-mercaptoethanol (LSB−) and loaded onto NuPAGE bis-Tris gels (Invitrogen). After separation, proteins were blotted onto polyvinylidene fluoride (PVDF) membranes. Western blot analysis was performed using a rabbit Gc peptide antiserum (9), a rabbit polyclonal antiserum against Gce (see above), the 4-D4 mouse anti-Gn monoclonal antibody (provided by Connie Schmaljohn, USAMRIID) (29), or a sheep polyclonal antiserum against RVFV (32) as the primary antibody and an appropriate peroxidase-conjugated secondary antibody. For dot blot analysis, samples containing RVFV$_{ns}$ particles were heated for 20 min at 80°C and spotted onto nitrocellulose membrane (Whatmann). The membrane was blocked with PBS containing 0.05% Tween 20 (vol/vol) and 5% Protifar (wt/vol; Nutricia). RVFV$_{ns}$ particles were detected using the 4-D4 anti-Gn monoclonal antibody.

Fusion at the plasma membrane. RVFV$_{ns}$ particles were allowed to bind to a confluent layer of BHK-21 cells on ice for 2 h. Cell-bound virus was subsequently exposed to prewarmed RPMI 1640 medium for 3 min at 37°C (water bath). The pH of the culture medium varied from pH 7.4 to

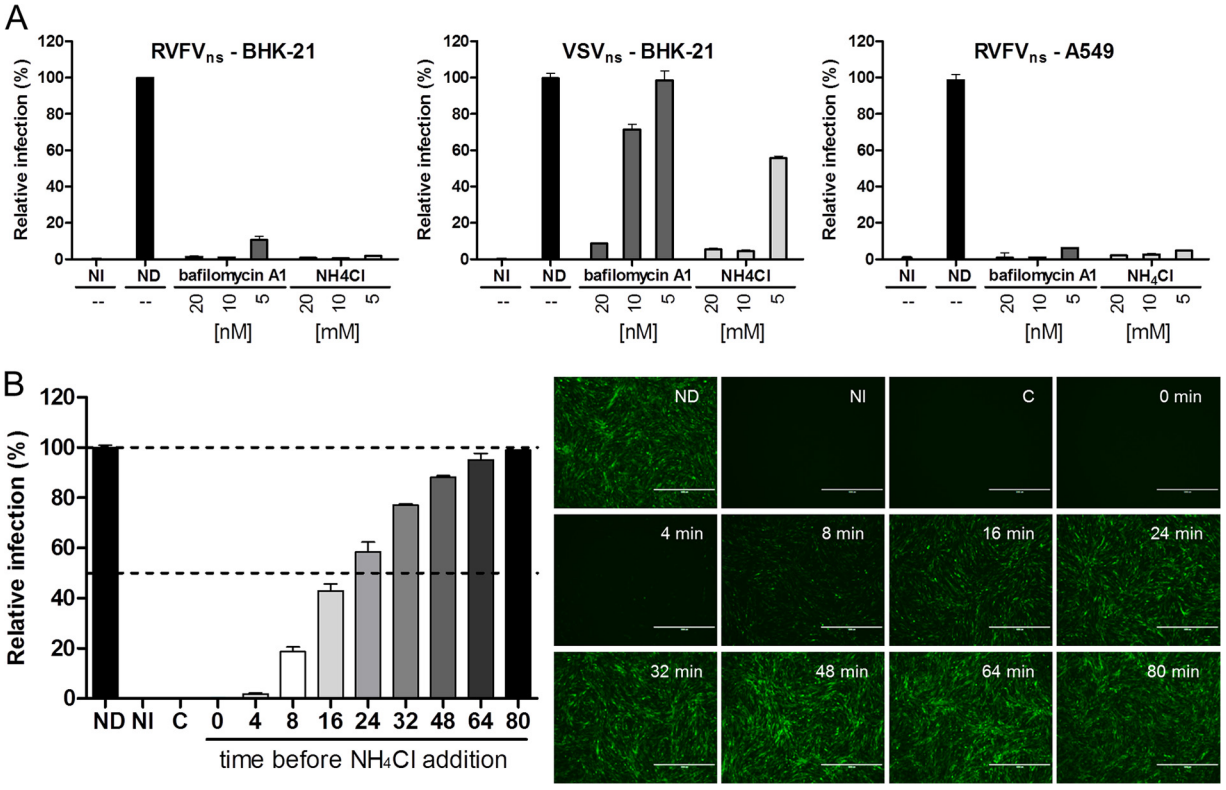

FIG 2 Entry of RVFV$_{ns}$ depends on vacuolar acidification. (A) BHK-21 or A549 cells were pretreated for 1 h with different concentrations of bafilomycin A1 or ammonium chloride (NH_4Cl) and subsequently infected with RVFV$_{ns}$ (MOI of ~0.1) or VSV$_{ns}$ (MOI of ~0.8). Infection (GFP-positive cells) was quantified by FACS. Results shown are representative of three individual experiments performed in duplicate. NI, not infected; ND, no drugs. (B) RVFV$_{ns}$ was bound to BHK-21 cells for 1 h in the cold and subsequently warmed to 37°C. NH_4Cl (10 mM) was added at indicated times to instantly raise the endosomal pH, thereby inhibiting further infection. Eighteen hours after warming, infection (GFP-positive cells) was analyzed by fluorescence microscopy (right panel; size bars represent 400 μM) and quantified by FACS (left panel). Untreated cells yielded ~70% infection. Graphical data shown are representative of two independent experiments performed in duplicate. C, NH_4Cl control (not infected).

5.0. The RPMI medium was replaced by culture medium containing bafilomycin A1 (20 nM), and cells were further incubated at 37°C, 5% CO_2. Twenty hours after the 3-min pH shock, infection (GFP-positive cells) was quantified by FACS and fluorescence microscopy.

Low-pH treatment of RVFV$_{ns}$ particles. RVFV$_{ns}$ particles in HNE buffer, pH 7.4, were exposed to conditions ranging from pH 7.4 to 5.0 by the addition of a pretitrated volume of 100 mM MES (morpholineethanesulfonic acid; pH 6.5 to 5.3) or 200 mM acetic acid (pH 5.0). The particles were incubated for 3 min at the desired pH at 37°C before the samples were back-neutralized to pH 7.4 with 0.1 N NaOH. Samples were subsequently used to infect BHK-21 cells, and the infections were analyzed 20 h.p.i. by FACS and fluorescence microscopy. To analyze the effect of low-pH treatment on the structural glycoproteins Gn and Gc, the pH of HNE-buffered RVFV$_{ns}$ particles was varied from pH 7.4 to 4.25 by the addition of MES (pH 6.5 to 5.3), 200 mM HAc (pH 5.0 to 4.75), or 500 mM HAc (pH 4.5 to 4.25). The RVFV$_{ns}$ particles were incubated for 0 to 10 min at 37°C, and the buffer was subsequently returned to pH 7.4 by adding a predetermined amount of 0.1 N NaOH or 0.5 N NaOH (pH 4.25). Samples were analyzed by Western blotting as described above.

DEPC treatment of RVFV$_{ns}$ particles. A diethylpyrocarbonate (DEPC) solution (1 M) in 96% ethanol was freshly prepared from a 1.12-g/ml commercial stock (Sigma). RVFV$_{ns}$ particles in PBS were incubated with various concentrations of DEPC as indicated for 10 min at 37°C. BHK-21 cells were inoculated with the treated virus for 20 h and assayed for infection (GFP-positive cells) by FACS and fluorescence microscopy.

Statistics. The data are representative of multiple independent experiments. Values are shown as means ± standard deviations (SD). Standard deviations were calculated using GraphPad Prism version 5.00 for Windows (GraphPad Software).

RESULTS

Entry of RVFV by endocytic uptake. We started our studies on RVFV cell entry with a limited pharmacological drug screen to investigate the uptake of the virus into cells using established inhibitors of cellular endocytic pathways. BHK-21 cells were pretreated for 1 h with different concentrations of drugs that interfere with dynamin-2- (dynasore), caveolin- (nystatin), clathrin- (chlorpromazine), or actin- (cytochalasin D) dependent endocytosis. Cells were then inoculated with nonspreading RVFV (RVFV$_{ns}$) at an MOI of ~0.4 in the presence of the drugs and subsequently incubated without the drugs but in the presence of bafilomycin A1 to inhibit further infection (Fig. 1A). A nonspreading recombinant of VSV (VSVΔG-GFP/G* [VSV$_{ns}$]) was used as a control virus (5). Both viruses express GFP from the viral genome, facilitating quantification of infection. Treatment of BHK-21 cells with dynasore or chlorpromazine, but not with the other compounds tested, reduced RVFV infection considerably, more strongly even than they affected VSV infection, which is well known to be dependent on dynamin-2 and clathrin during entry (Fig. 1A). The presence of these drugs did not have a significant effect on the cell viability (Fig. 1B). Importantly, infection of RVFV$_{ns}$ was hardly affected if dynasore or chlorpromazine was

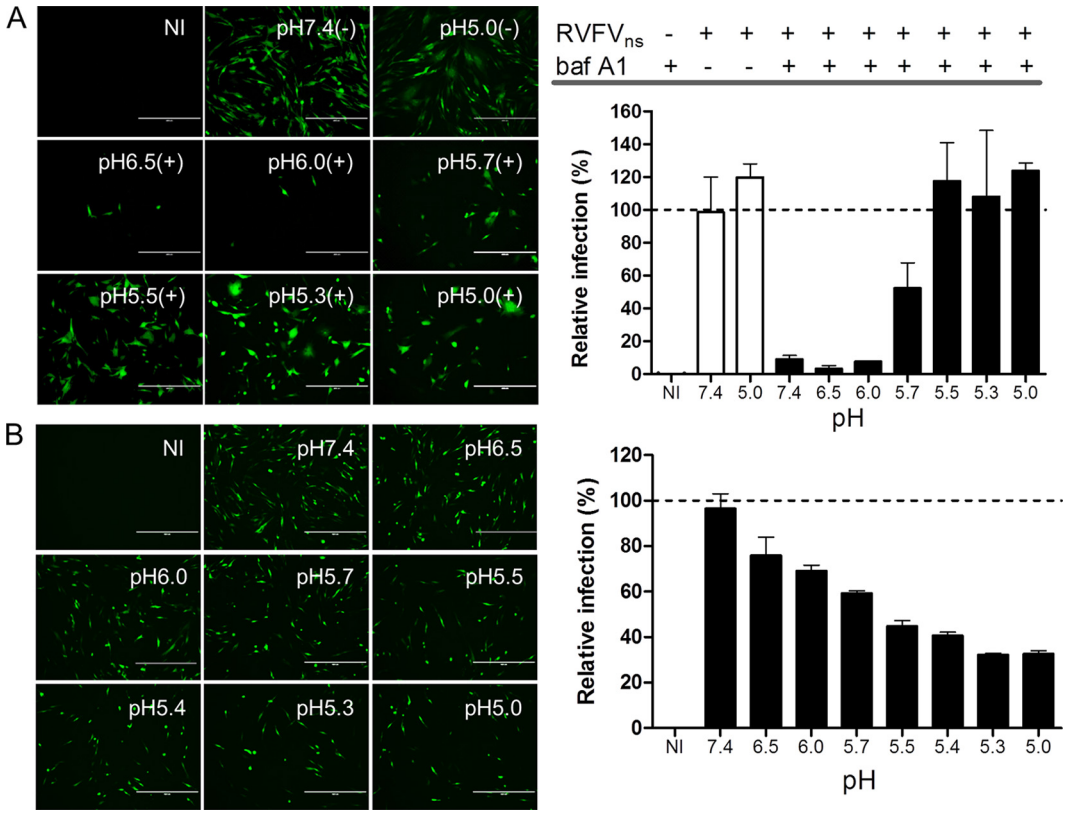

FIG 3 Low-pH-activated penetration of cell-bound RVFV$_{ns}$ and inactivation of unbound RVFV$_{ns}$ particles. (A) RVFV$_{ns}$ was allowed to bind in the cold to a confluent monolayer of BHK-21 cells for 2 h before the cell-bound virus was exposed for 3 min at 37°C to the indicated pH. Infection was continued in culture medium containing bafilomycin A1 (baf A1; 20 nM) to inhibit infection via the endocytic route. Infection (GFP-positive cells) was analyzed 20 h after warming by fluorescence microscopy and was quantified by FACS. Untreated cells (pH 7.4) yielded ~40% infection. The results shown are representative of two individual experiments performed in triplicate. (B) RVFV$_{ns}$ particles were incubated at the indicated pH for 3 min at 37°C. After neutralization of the medium, infectivity of the virus was assayed on BHK-21 cells. Infection (GFP-positive cells) was analyzed 20 h.p.i. by fluorescence microscopy (left panel; size bars represent 400 μM) and quantified by FACS (right panel). Virus incubated at neutral pH resulted in ~30% GFP-positive cells. Graphical data shown are representative of four individual experiments performed in duplicate. The controls in the experiments whose results are shown in panels A and B were cells that were not infected (NI).

added 2 h postinoculation, indicating that the drugs only affect the entry stage of infection (Fig. 1C). Similar effects of dynasore and chlorpromazine on RVFV$_{ns}$ infection were seen on A549 cells (data not shown). We confirmed the involvement of dynamin-2 in RVFV$_{ns}$ entry on BHK-21 cells using a novel and potent inhibitor of dynamin-2 named dyngo-4a (23) (Fig. 1B and D). Dynasore and chlorpromazine also strongly inhibited entry of a recombinant RVFV, RVFV$_{rec}$, expressing GFP (Fig. 1E). These drug inhibition data indicate that entry of RVFV is sensitive to inhibitors which interfere with dynamin-2 and clathrin-dependent endocytosis.

RVFV entry depends on vacuolar acidification. Previously, it was described that low-pH incubation of cells overexpressing the RVFV glycoproteins resulted in extensive cell-cell fusion, suggesting that after endocytosis, RVFV fusion is activated by the acidic environment of endosomal compartments (11, 37). To explore the requirements of a low endosomal pH for virus entry, we analyzed the infection of RVFV$_{ns}$ in the presence of the lysosomotropic agents bafilomycin A1, an inhibitor of vacuolar-type H^+-ATPase proton pumps, and the lipophilic weak base ammonium chloride (NH_4Cl), both of which prevent acidification of endosomal compartments. VSV$_{ns}$, known to be acid activated in early endosomes with a pH threshold of pH 6.1 (35, 68), was used as a control. The results demonstrate that RVFV$_{ns}$ entry is strictly dependent on vacuolar acidification, as infection of BHK-21 and A549 cells was inhibited by bafilomycin A1, as well as by NH_4Cl (Fig. 2A). Compared to VSV$_{ns}$, RVFV$_{ns}$ appears to be more sensitive to the lysosomotropic agents, suggesting that the virus has a lower pH threshold for activation and therefore may be activated in more-acidic vacuoles beyond the early endosomal compartments.

To define the time of acid exposure after receptor binding, we used a previously described NH_4Cl add-in experiment (40). The addition of NH_4Cl to the medium is known to almost instantly raise the endosomal pH (43), allowing studies of the kinetics by which viruses pass the acid-requiring entry step after binding. We synchronized the infection of RVFV$_{ns}$ by allowing the virus to bind to cells in the cold. After removal of the unbound virus, we rapidly transferred the cells to 37°C and added 10 mM NH_4Cl at different times after warming. About 90% of the virus experienced the acid-dependent step between 4 and 48 min after warming of the cells (Fig. 2B). The entry kinetics of RVFV$_{ns}$ are similar to those reported for the *Phlebovirus* UUKV (39) and influenza viruses (40), which were both shown to fuse at low pH in late endosomal or lysosomal compartments (38, 39, 69).

RVFV fusion occurs under acidic conditions that resemble the endolysosomal compartments. To determine the pH thresh-

old for fusion of RVFV, we measured infection after low-pH-induced fusion at the plasma membrane under conditions where acidification of endosomes—and normal virus entry—is blocked by bafilomycin A1. In this acid-mediated endocytosis bypass experiment, which was previously described for SFV and UUKV (19, 39), $RVFV_{ns}$ particles were bound to cells in the cold and subsequently exposed for 3 min at 37°C to media with various pHs. The medium was replaced with culture medium containing bafilomycin A1 to inhibit further infection via the endocytic pathway. The results demonstrate that treatment of the cell-bound virus at or below pH 5.5 fully bypassed the requirement for vacuolar acidification (Fig. 3A). The bypass was less efficient at pH 5.7, and only limited infection was observed at pH 6 or higher, indicating that the pH threshold for RVFV membrane fusion is around pH 5.7. Exposure of free $RVFV_{ns}$ particles to low pH (pH 6.5 to 5) for 3 min did reduce virus infectivity, although virus inactivation was not complete (Fig. 3B).

Acid-induced rearrangement of the Gc into higher-order structures. Next, we examined the effects of exposure to low pH on the structural organization of the RVFV envelope glycoproteins. $RVFV_{ns}$ particles were incubated in buffers of low pH for 10 min. After neutralization of the buffers, viral proteins were analyzed by Western blotting performed under nonreducing conditions. The Gn and Gc glycoproteins, as well as the 78-kDa protein, were detected using a polyclonal RVFV antiserum, a Gn-specific monoclonal antibody, and a Gc-specific peptide antiserum (Fig. 4A). Incubation of $RVFV_{ns}$ under the low-pH conditions that activate virus entry (pH < 6) (Fig. 3A) led to the disappearance of the Gc monomer and the concomitant appearance of a more slowly migrating protein moiety. Incubation at low pH did not influence migration of the Gn or the 78-kDa protein. The disappearance of the Gc monomer suggested that the slowly migrating band consists of an oligomer of Gc which can be detected by the polyclonal RVFV antiserum but, perhaps through epitope inaccessibility, not by the Gc peptide antiserum. Consistent with this notion, heating of acid-activated $RVFV_{ns}$ to 90°C resulted in the disappearance of the slowly migrating band and the simultaneous appearance of monomeric Gc (Fig. 4B). To further study the identity of the presumed Gc oligomer, we produced a polyclonal antiserum by inoculating rabbits with the ectodomain of Gc produced using the *Drosophila* expression system. This antiserum efficiently recognized the monomeric and the more slowly migrating form of Gc on Western blots, confirming the identity of the Gc oligomer (Fig. 4C). Using this antiserum, we analyzed the kinetics of Gc oligomer formation. The conversion of Gc into SDS-stable oligomers slowly increased with time of pH treatment (Fig. 4C). Conversion became detectable already after 15 s and was nearly complete after 4 min of incubation at low pH. These results demonstrate that incubation of RVFV at the fusion-activating pH triggers a structural reorganization of Gc from an apparently metastable to a highly stable oligomeric conformation, reminiscent of the stable acid-activated trimeric class II fusion proteins of alpha- and flaviviruses (31, 59, 64).

RVFV entry is inhibited by substitution of a single histidine in Gc. Protonation of one or more histidines can be crucial for triggering conformational changes in viral fusion proteins (28). A first clue for a pH-sensing role of histidines in RVFV infection came from the observation that preincubation of $RVFV_{ns}$ with diethylpyrocarbonate (DEPC), a chemical which specifically modifies the aromatic ring of histidines, preventing its protonation (7), clearly inhibits RVFV infection of BHK-21 cells in a concentration-dependent manner (Fig. 5A). To further study the role of histidine protonation in virus entry, we identified and replaced eight conserved histidines in Gn and Gc (Table 1 and Fig. 5B) with

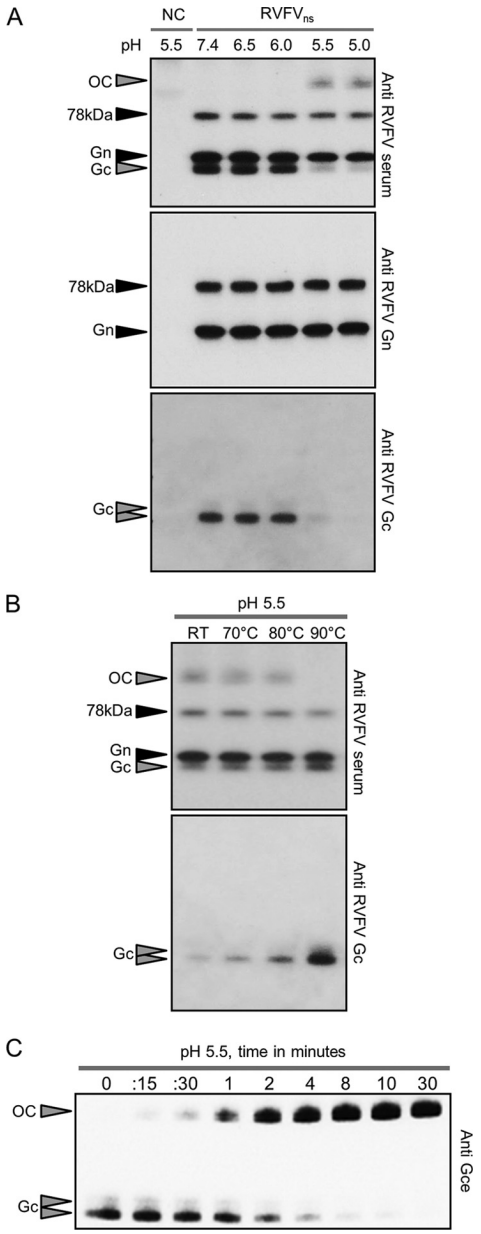

FIG 4 Acid exposure triggers the formation of an SDS- and temperature-resistant Gc oligomer. (A) $RVFV_{ns}$ particles were exposed to the indicated pHs for 10 min at 37°C, returned to neutral pH, and subsequently analyzed by Western blotting performed under nonreducing conditions. RVFV glycoproteins were detected with an RVFV antiserum, a monoclonal antibody against Gn, or a polyclonal anti-Gc peptide antiserum. In some cases, Gc migrates as a closely spaced doublet. (B) $RVFV_{ns}$ particles were exposed for 10 min to pH 5.5 at 37°C, returned to neutral pH, and heated for 20 min at the indicated temperatures. Samples were subsequently analyzed by Western blotting (nonreducing conditions) using an RVFV antiserum or an anti-Gc peptide antiserum. (C) $RVFV_{ns}$ particles were exposed to pH 5.5 at 37°C for the indicated times and analyzed by Western blotting (nonreducing conditions) using a polyclonal antiserum raised against the purified Gc ectodomain (Gce). OC, oligomeric complex; NC, negative control (medium from mock-transfected replicon cells); RT, room temperature.

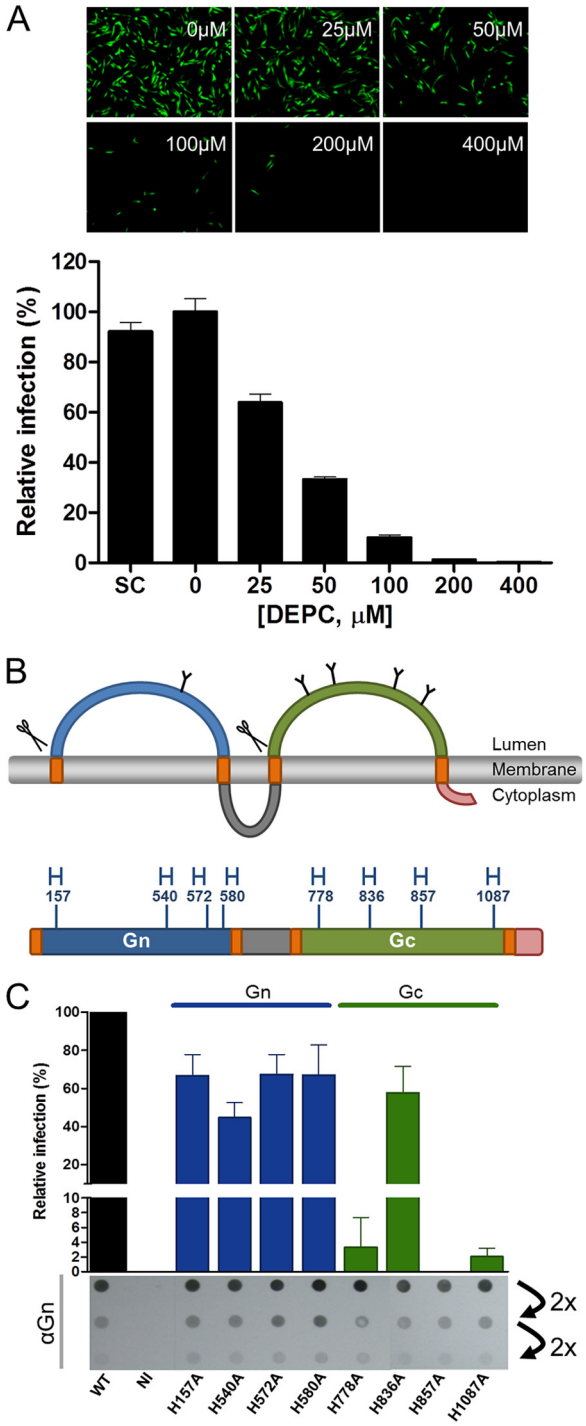

FIG 5 Role of histidines in $RVFV_{ns}$ infectivity. (A) $RVFV_{ns}$ was pretreated with different concentrations of DEPC for 10 min at 37°C and subsequently assayed for infectivity. Infectivity (GFP-positive cells) was analyzed 20 h postinoculation by fluorescence microscopy and quantified by FACS. BHK-21 cells inoculated with virus treated with 0 μM DEPC yielded ~20% infection. Graphical data shown are representative of two independent experiments performed in triplicate. SC, solvent control (0.2% ethanol). (B) Membrane topology of the RVFV M segment-encoded polyprotein starting from the fourth methionine (16). The predicted N-linked glycosylation sites (Y symbols) and signal peptidase cleavage sites (scissors) are indicated. The luminal domains of Gn and Gc and the cytoplasmic domains of Gn and Gc are colored in blue, green, gray, and pink, respectively. The orange blocks represent the transmembrane-spanning regions. The positions and amino acid numbering of conserved histidines (H), calculated from the first methionine (GenBank sequence accession number JF784387), are indicated in the linear diagram of the GnGc polyprotein. (C) Wild-type (WT) $RVFV_{ns}$ and mutants containing histidine-to-alanine substitutions, used in equal amounts as determined by a dot blot assay (2-fold dilutions of viruses are shown), were analyzed for their infectivity on BHK-21 cells. BHK-21 cells inoculated with wild-type $RVFV_{ns}$ particles resulted in ~20% infection. Infection (GFP-positive cells) was quantified by FACS. Noninfected (NI) BHK-21 cells were included as a negative control. The data shown represent the combined results for three independently produced batches of wild-type and mutant $RVFV_{ns}$ particles tested in independent experiments, each performed in triplicate.

the small and nonpolar amino acid alanine. $RVFV_{ns}$ particles carrying the histidine-to-alanine replacements were produced and secreted from BHK-21 replicon cells (33) with efficiencies resembling that of wild-type $RVFV_{ns}$, indicating that the mutations in Gn and Gc did not impair the assembly and release of virus particles (data not shown). The amounts of mutant and wild-type virus particles were normalized using a dot blot assay, and equal virus quantities were compared for their relative infectivities (Fig. 5C). $RVFV_{ns}$ mutants with histidine-to-alanine substitutions in Gn were all viable, although their infectivity was slightly reduced. In contrast, three of the four histidine-to-alanine substitutions in Gc either completely abolished (H857A mutant) or strongly impaired infectivity (H778A and H1087A mutants), to less than 5% relative to that of wild-type $RVFV_{ns}$.

H857 is essential for acid-induced rearrangement of Gc into higher-order structures. Next, we analyzed the effects of the histidine-to-alanine mutations on the formation, stability, and conversion kinetics of the Gc oligomer. Acid exposure of similar amounts of mutant and wild-type $RVFV_{ns}$ particles resulted in the formation of the SDS-resistant Gc oligomer in all mutants, with the exception of the H857A mutant (Fig. 6A, upper left). The Gc oligomers of the H778A, H836A, and H1087A mutants were not stable at 80°C, in contrast to those of the wild type and the Gn histidine mutants (Fig. 6A, lower left). To analyze their thermostability in more detail, the Gc oligomers were subjected to heating at different temperatures prior to Western blot analysis. Compared to the wild-type oligomer, the Gc oligomers of the H778A, H836A, and H1087A mutants appeared slightly less thermostable and dissociated at 80°C but not at 70°C (Fig. 6A, right). Next, we used Western blotting to assess the effects of the mutations on the kinetics of the Gc conversion into the SDS-stable oligomer upon acid exposure (Fig. 6B). The conversion kinetics of the Gc H778A, H836A, and H1087A mutants upon pH treatment appeared grossly similar to that of the wild type (Fig. 6B). Clearly, acid exposure of the Gc mutant carrying the lethal H857A substitution even up to 30 min did not allow the formation of the SDS-resistant Gc oligomer (Fig. 6B), suggesting that the formation of the stable Gc oligomer induced by protonation of histidine 857 is essential for virus entry into the host cell. Finally, to assess a possible shift in the pH activation threshold, we analyzed the Gc conversion for the H857A Gc mutant and wild-type $RVFV_{ns}$ particles at pH values below pH 5.5. Incubation under these acidic conditions for 10 min at 37°C resulted in the formation of the stable oligomer in wild-type $RVFV_{ns}$ particles. In contrast, no stable Gc oligomer was observed after treatment of $RVFV_{ns}$ particles containing the H857A mutation (Fig. 6C).

TABLE 1 Conservation of the selected histidines in the RVFV Gn and Gc glycoproteins among members of the *Phlebovirus* genus of the *Bunyaviridae* family as determined by ClustalW alignment

	Amino acid at indicated position[a] in:							
	Gn protein				Gc protein			
Phlebovirus (GenBank accession no.)	157	540	572	580	778	836	857	1087
Rift Valley fever virus (JF784387)	H	H	H	H	H	H	H	H
Sandfly fever Naples virus (YP089671)	H	H	H	H	H	H	H	H
Toscana virus (ABS85173)	H	H	H	H	H	H	H	H
Massilia virus (ACI24011)	H	H	H	H	H	H	H	H
Echarate virus (HM119411)	H	Y	Y	H	H	H	H	H
Turuna virus (HM119432)	H	H	N	H	H	H	H	H
Chandiru virus (HM119408)	H	H	N	H	H	H	H	H
Mucura virus (HM119420)	H	H	Q	H	H	H	H	H
Ariquemes virus (HM119405)	H	H	S	H	H	H	H	H
Morumbi virus (HM119423)	H	H	T	H	H	H	H	H
Alenquer virus (HM119402)	H	H	K	H	H	H	H	H
Itaituba virus (HM119417)	H	H	K	H	H	H	H	H
Serra Norte virus (HM119429)	H	Y	K	H	H	H	H	H
Nique virus (HM119426)	H	H	N	H	H	H	H	H
Oriximina virus (HM119435)	H	Y	H	H	H	H	H	H
Jacunda virus (HM466935)	H	Y	Y	H	H	H	H	H
Sandfly fever Sicilian virus (AAA75043)	H	H	E	H	R	H	H	H
Punta Toro virus (ABD92923)	H	H	H	H	H	H	H	H
Severe fever with thrombocytopenia syndrome virus (HM745931)	—	H	E	Y	R	R	P	S
Uukuniemi virus (AAA79512)	—	R	A	F	H	R	Y	H

[a] Amino acid numbers correspond to the RVFV M-segment encoding polyprotein. —, ClustalW alignment displays a gap at this position.

DISCUSSION

It is well established that bunyaviruses require the acidic pH found in endosomes to activate fusion, but it remains unclear how fusion is mediated at the molecular level. In this study, we demonstrate that exposure of RVFV particles to acidic pH converts the viral Gc protein into a highly stable oligomer. The pH required for this major conformational change correlates with the pH threshold required to activate fusion of virus particles at the plasma membrane. Mutagenesis of conserved histidines in the viral glycoproteins identified a single histidine in Gc that was strictly required for entry, as well as for the acid-induced conversion of Gc into its stable oligomeric form. These data provide new insight into the molecular basis of acid-activated bunyavirus fusion.

Most bunyaviruses studied to date utilize clathrin-mediated endocytosis to gain access to the cell interior (22, 25, 38, 39, 55, 58). For UUKV, a clathrin-independent pathway has been suggested as an alternative route (39). We demonstrate here that RVFV entry is sensitive to drugs perturbing the function of clathrin and dynamin, which is consistent with entry via a clathrin-mediated endocytic pathway. Further studies are required to confirm this assumption. Upon endocytosis, RVFV particles are transported deep into the cell through maturing endosomes. The pH threshold (pH < 6) required for virus fusion at the plasma membrane and rearrangement of Gc suggests that fusion of RVFV occurs in late endosomes. This late penetration is consistent with the time at which 50% of the total amount of infection has been reached (half-time) of RVFV of ~20 min during which the virus undergoes its acid-activating step. Similar pH thresholds and penetration kinetics have been observed for UUKV, another *Phlebovirus* (39). Our data indicate that RVFV can be classified as a late-penetrating virus (38).

Exposure to low pH converts the $RVFV_{ns}$ Gc protein from an apparently metastable to a highly stable oligomeric conformation. Similar pH-induced rearrangements have been reported for envelope glycoproteins of other bunyaviruses. These conformational changes have variously been shown to lead to dissociation of the Gn-Gc heterodimer (Hantavirus), to changes in the Gc antigenic structure, or to alteration in the cleavage pattern after proteolytic processing of the Gc protein (UUKV and La Crosse virus) (16, 21, 52). The low-pH-induced changes in the glycoprotein shell of UUKV virions have been visualized nicely by electron microscopy, revealing the flattening of the glycoprotein capsomers (44, 52). Low-pH incubation of La Crosse virus and UUKV leads to virus aggregation (44, 66). Activation of fusion proteins generally triggers the exposure of a hydrophobic "fusion peptide" which normally functions by inserting into the host membrane and initiating fusion, which might explain the observed acid-induced virus aggregation. Typically, fusion proteins are trimeric in this fusion-active state (8, 17). Hence, we assume that the RVFV Gc stable oligomer is also made up of three Gc molecules, but further research is needed to confirm this hypothesis.

The acid-induced Gc oligomer displays a remarkable resistance to temperature dissociation and SDS detergent denaturation (10). In agreement with these observations, back-neutralization of the acid-exposed virus particles did not reverse the transition of Gc into a stable oligomer. In general, viral fusion proteins convert to a stable form during fusion, thereby generating the energy needed for membrane coalescence. For class I and II viral fusion proteins, this transition was shown to be irreversible (51). Intriguingly, exposure of virus to the activating pH in the absence of target membranes also fully converts Gc into the stable oligomer; however, although a reduction is seen, it does not completely inactivate virus infectivity even after incubation times of up to 16 min (data not shown). It remains to be seen whether the stable Gc oligomer represents the final postfusion form of the Gc fusion protein or

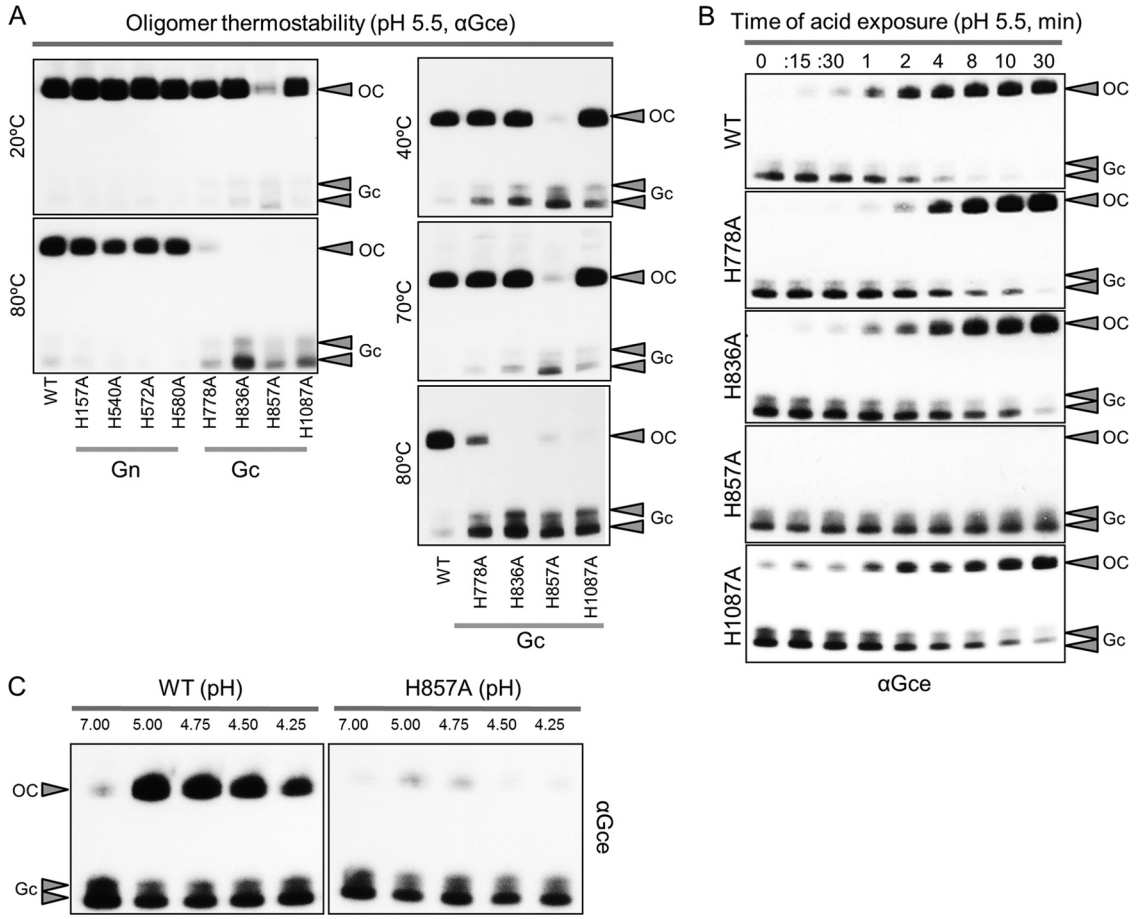

FIG 6 Effects of histidine substitutions in RVFV glycoproteins on the formation and stability of the Gc oligomer. (A) Equal amounts of wild-type and mutant $RVFV_{ns}$ particles were exposed for 10 min to pH 5.5 at 37°C, returned to neutral pH, heated for 20 min at the indicated temperatures, and subsequently analyzed by Western blotting (nonreducing conditions) using a polyclonal antiserum raised against the Gc ectodomain (Gce). In some cases, Gc runs as a closely spaced doublet. The thermostability of the acid-induced Gc oligomer is indicated for the wild-type and Gn- and Gc-His mutant $RVFV_{ns}$ particles at 20°C and 80°C (left) or for the wild-type and the Gc-His mutant $RVFV_{ns}$ particles at 40°C, 70°C, and 80°C (right). (B) Equal amounts of wild-type and mutant $RVFV_{ns}$ particles containing histidine-to-alanine mutations in Gc were exposed to pH 5.5 at 37°C for the indicated times and analyzed by Western blotting (nonreducing conditions) using a polyclonal antiserum raised against the Gc ectodomain. OC, oligomeric complex; WT, wild-type. (C) Equal amounts of wild-type and H857A mutant $RVFV_{ns}$ particles were exposed for 10 min at 37°C to the indicated pH. The Gc conversion was analyzed by Western blotting as described for panel B.

represents a crucial intermediate which awaits further reorganization. In the latter situation, alternative factors (e.g., interaction with the target membrane) may be required to drive the conformational rearrangements to completion.

In the RVFV virion, Gc is organized as a heterodimer together with Gn (24). The Gn-Gc heterodimer is the building block of 110 hexamers and 12 pentamers containing six and five of the Gn-Gc heterodimeric units, respectively. Together, these 122 capsomers make up the icosahedral shell of the virion, following a T = 12 triangulation (13, 24). Exposure of virions to the activating pH will lead to rearrangement of the metastable Gn-Gc heterodimer and concomitantly enforce the interactions between Gc subunits, resulting in the formation of a Gc homooligomer. Exposure of virions to the acidic pH of 6 did not have any impact on the structure of RVFV particles as shown by cryoelectron tomography, consistent with the fusion-activating pH threshold of below 6 that we observed (24). It will be interesting to investigate how the Gc protomers in the virions—organized as pentamers and hexameric Gn-Gc heterodimers—collectively undergo the structural transition toward the (presumably) trimeric Gc oligomer after exposure to the activating pH.

Protonation of histidines in Gc may play a key role at different stages of the fusion process. The inability of the H857A mutant to form stable Gc oligomers, in combination with its abrogated entry function, suggests that Gc oligomerization is essential for virus entry and that protonation of H857 plays a crucial role in this process. In addition, the substitution of H778 and H1087 in Gc has a severe effect on virus entry, yet Gc oligomerization still occurred and the temperature stability was only marginally affected. This suggests that formation of the Gc oligomer, although required, may not be sufficient for inducing fusion. We speculate that the single mutations may impair a later step in the fusion reaction (36). The H778, H857, and H1087 histidines in Gc may collectively contribute to pH sensing, initiation, and propagation of conformational rearrangements toward the postfusion structure. Further interpretation of the consequences of the histidine substitutions awaits the elucidation of the high-resolution structures of the Gc protein in its pre- and postfusion states.

ACKNOWLEDGMENTS

We thank Rianka Vloet and Nadia Oreshkova (Central Veterinary Institute, Lelystad, The Netherlands) for their assistance. We thank Christiaan Potgieter (ARC-OVI) for providing the 841 antiserum. We thank Sean Whelan and Matthijs Raaben (Harvard Medical School, Boston, MA) for providing the VSVΔG-GFP recombinant virus. We thank Connie Schmaljohn (USAMRIID, Fort Detrick, MD) for providing the 4-D4 monoclonal antibody recognizing Gn.

This work was supported by the Dutch Ministry of Economic Affairs, Agriculture and Innovation, project codes KB-12-004.02-002 and BO-10-001-211.

REFERENCES

1. **Arikawa J, Takashima I, Hashimoto N.** 1985. Cell fusion by haemorrhagic fever with renal syndrome (HFRS) viruses and its application for titration of virus infectivity and neutralizing antibody. Arch. Virol. **86**: 303–313.
2. **Balkhy HH, Memish ZA.** 2003. Rift Valley fever: an uninvited zoonosis in the Arabian peninsula. Int. J. Antimicrob. Agents **21**:153–157.
3. **Boo I, KteWierik Douam F, Lavillette D, Poumbourios P, Drummer HE.** 2012. Distinct roles in folding, CD81 receptor binding and viral entry for conserved histidine residues of hepatitis C virus glycoprotein E1 and E2. Biochem. J. **443**:85–94.
4. **Carneiro FA, et al.** 2003. Membrane fusion induced by vesicular stomatitis virus depends on histidine protonation. J. Biol. Chem. **278**:13789–13794.
5. **Chandran K, Sullivan NJ, Felbor U, Whelan SP, Cunningham JM.** 2005. Endosomal proteolysis of the Ebola virus glycoprotein is necessary for infection. Science **308**:1643–1645.
6. **Chanel-Vos C, Kielian M.** 2006. Second-site revertants of a Semliki Forest virus fusion-block mutation reveal the dynamics of a class II membrane fusion protein. J. Virol. **80**:6115–6122.
7. **Chang LH, Tam MF.** 1993. Site-directed mutagenesis and chemical modification of histidine residues on an alpha-class chick liver glutathione S-transferase CL 3-3. Histidines are not needed for the activity of the enzyme and diethylpyrocarbonate modifies both histidine and lysine residues. Eur. J. Biochem. **211**:805–811.
8. **Cosset FL, Lavillette D.** 2011. Cell entry of enveloped viruses. Adv. Genet. **73**:121–183.
9. **de Boer SM, et al.** 2010. Rift Valley fever virus subunit vaccines confer complete protection against a lethal virus challenge. Vaccine **28**:2330–2339.
10. **Fass D.** 2003. Conformational changes in enveloped virus surface proteins during cell entry. Adv. Protein Chem. **64**:325–362.
11. **Filone CM, Heise M, Doms RW, Bertolotti-Ciarlet A.** 2006. Development and characterization of a Rift Valley fever virus cell-cell fusion assay using alphavirus replicon vectors. Virology **356**:155–164.
12. **Findlay GM, Daubney R.** 1931. The virus of Rift Valley fever or enzoötic hepatitis. Lancet **ii**:1350–1351.
13. **Freiberg AN, Sherman MB, Morais MC, Holbrook MR, Watowich SJ.** 2008. Three-dimensional organization of Rift Valley fever virus revealed by cryoelectron tomography. J. Virol. **82**:10341–10348.
14. **Fritz R, Stiasny K, Heinz FX.** 2008. Identification of specific histidines as pH sensors in flavivirus membrane fusion. J. Cell Biol. **183**:353–361.
15. **Garry CE, Garry RF.** 2004. Proteomics computational analyses suggest that the carboxyl terminal glycoproteins of Bunyaviruses are class II viral fusion protein (beta-penetrenes). Theor. Biol. Med. Model. **1**:10. doi: 10.1186/1742-4682-1-10.
16. **Gonzalez-Scarano F.** 1985. La Crosse virus G1 glycoprotein undergoes a conformational change at the pH of fusion. Virology **140**:209–216.
17. **Harrison SC.** 2008. Viral membrane fusion. Nat. Struct. Mol. Biol. **15**: 690–698.
18. **Hartley DM, et al.** 2011. Potential effects of Rift Valley fever in the United States. Emerg. Infect. Dis. **17**:e1. doi:10.3201/eid1708.101088.
19. **Helenius A, Kartenbeck J, Simons K, Fries E.** 1980. On the entry of Semliki forest virus into BHK-21 cells. J. Cell Biol. **84**:404–420.
20. **Hepojoki J, Strandin T, Lankinen H, Vaheri A.** 2012. Hantavirus structure—molecular interactions behind the scene. J. Gen. Virol. **93**(Pt 8): 1631–1644.
21. **Hepojoki J, Strandin T, Vaheri A, Lankinen H.** 2010. Interactions and oligomerization of hantavirus glycoproteins. J. Virol. **84**:227–242.
22. **Hollidge BS, et al.** 2012. Orthobunyavirus entry into neurons and other mammalian cells occurs via clathrin-mediated endocytosis and requires trafficking into early endosomes. J. Virol. **86**:7988–8001.
23. **Howes MT, et al.** 2010. Clathrin-independent carriers form a high capacity endocytic sorting system at the leading edge of migrating cells. J. Cell Biol. **190**:675–691.
24. **Huiskonen JT, Overby AK, Weber F, Grunewald K.** 2009. Electron cryo-microscopy and single-particle averaging of Rift Valley fever virus: evidence for GN-GC glycoprotein heterodimers. J. Virol. **83**:3762–3769.
25. **Jin M, et al.** 2002. Hantaan virus enters cells by clathrin-dependent receptor-mediated endocytosis. Virology **294**:60–69.
26. **Kadlec J, Loureiro S, Abrescia NG, Stuart DI, Jones IM.** 2008. The postfusion structure of baculovirus gp64 supports a unified view of viral fusion machines. Nat. Struct. Mol. Biol. **15**:1024–1030.
27. **Kakach LT, Wasmoen TL, Collett MS.** 1988. Rift Valley fever virus M segment: use of recombinant vaccinia viruses to study Phlebovirus gene expression. J. Virol. **62**:826–833.
28. **Kampmann T, Mueller DS, Mark AE, Young PR, Kobe B.** 2006. The role of histidine residues in low-pH-mediated viral membrane fusion. Structure **14**:1481–1487.
29. **Keegan K, Collett MS.** 1986. Use of bacterial expression cloning to define the amino acid sequences of antigenic determinants on the G2 glycoprotein of Rift Valley fever virus. J. Virol. **58**:263–270.
30. **Kielian M.** 2006. Class II virus membrane fusion proteins. Virology **344**: 38–47.
31. **Kielian M, Rey FA.** 2006. Virus membrane-fusion proteins: more than one way to make a hairpin. Nat. Rev. Microbiol. **4**:67–76.
32. **Kortekaas J, et al.** 2010. Intramuscular inoculation of calves with an experimental Newcastle disease virus-based vector vaccine elicits neutralizing antibodies against Rift Valley fever virus. Vaccine **28**:2271–2276.
33. **Kortekaas J, et al.** 2011. Creation of a nonspreading Rift Valley fever virus. J. Virol. **85**:12622–12630.
34. **Krishnan A, et al.** 2009. A histidine switch in hemagglutinin-neuraminidase triggers paramyxovirus-cell membrane fusion. J. Virol. **83**: 1727–1741.
35. **Le Blanc I, et al.** 2005. Endosome-to-cytosol transport of viral nucleocapsids. Nat. Cell Biol. **7**:653–664.
36. **Li Z, Blissard GW.** 2011. Autographa californica multiple nucleopolyhedrovirus GP64 protein: roles of histidine residues in triggering membrane fusion and fusion pore expansion. J. Virol. **85**:12492–12504.
37. **Liu L, Celma CC, Roy P.** 2008. Rift Valley fever virus structural proteins: expression, characterization and assembly of recombinant proteins. Virol. J. **5**:82.
38. **Lozach PY, Huotari J, Helenius A.** 2011. Late-penetrating viruses. Curr. Opin. Virol. **1**:35–43.
39. **Lozach PY, et al.** 2010. Entry of bunyaviruses into mammalian cells. Cell Host Microbe **7**:488–499.
40. **Martin K, Helenius A.** 1991. Transport of incoming influenza virus nucleocapsids into the nucleus. J. Virol. **65**:232–244.
41. **Mundel B, Gear J.** 1951. Rift valley fever. I. The occurrence of human cases in Johannesburg. S. Afr. Med. J. **25**:797–800.
42. **Ogino M, et al.** 2004. Cell fusion activities of Hantaan virus envelope glycoproteins. J. Virol. **78**:10776–10782.
43. **Ohkuma S, Poole B.** 1978. Fluorescence probe measurement of the intralysosomal pH in living cells and the perturbation of pH by various agents. Proc. Natl. Acad. Sci. U. S. A. **75**:3327–3331.
44. **Overby AK, Pettersson RF, Grunewald K, Huiskonen JT.** 2008. Insights into bunyavirus architecture from electron cryotomography of Uukuniemi virus. Proc. Natl. Acad. Sci. U. S. A. **105**:2375–2379.
45. **Overby AK, Pettersson RF, Neve EP.** 2007. The glycoprotein cytoplasmic tail of Uukuniemi virus (Bunyaviridae) interacts with ribonucleoproteins and is critical for genome packaging. J. Virol. **81**:3198–3205.
46. **Pepin M, Bouloy M, Bird BH, Kemp A, Paweska J.** 2010. Rift Valley fever virus (Bunyaviridae: Phlebovirus): an update on pathogenesis, molecular epidemiology, vectors, diagnostics and prevention. Vet. Res. **41**:61.
47. **Piper ME, Sorenson DR, Gerrard SR.** 2011. Efficient cellular release of Rift Valley fever virus requires genomic RNA. PLoS One **6**:e18070. doi: 10.1371/journal.pone.0018070.
48. **Plassmeyer ML, et al.** 2007. Mutagenesis of the La Crosse virus glycoprotein supports a role for Gc (1066–1087) as the fusion peptide. Virology **358**:273–282.
49. **Qin ZL, Zheng Y, Kielian M.** 2009. Role of conserved histidine residues

in the low-pH dependence of the Semliki Forest virus fusion protein. J. Virol. **83**:4670–4677.
50. **Rich KM, Wanyoike F.** 2010. An assessment of the regional and national socio-economic impacts of the 2007 Rift Valley fever outbreak in Kenya. Am. J. Trop. Med. Hyg. **83**:52–57.
51. **Roche S, Albertini AA, Lepault J, Bressanelli S, Gaudin Y.** 2008. Structures of vesicular stomatitis virus glycoprotein: membrane fusion revisited. Cell. Mol. Life Sci. **65**:1716–1728.
52. **Ronka H, Hilden P, Von Bonsdorff CH, Kuismanen E.** 1995. Homodimeric association of the spike glycoproteins G1 and G2 of Uukuniemi virus. Virology **211**:241–250.
53. **Rusu M, et al.** 2012. An assembly model of Rift Valley fever virus. Front. Microbiol. **3**:254.
54. **Sanchez-San Martin C, Liu CY, Kielian M.** 2009. Dealing with low pH: entry and exit of alphaviruses and flaviviruses. Trends Microbiol. **17**:514–521.
55. **Santos RI, et al.** 2008. Oropouche virus entry into HeLa cells involves clathrin and requires endosomal acidification. Virus Res. **138**:139–143.
56. **Schmaljohn CS, Nichol ST.** 2007. Bunyaviridae, p 1741–1789. *In* Knipe DM, Howley PM (ed), Fields virology, 5th ed, **vol 2**. Lippincott Williams & Wilkins, Philadelphia, PA.
57. **Schowalter RM, Chang A, Robach JG, Buchholz UJ, Dutch RE.** 2009. Low-pH triggering of human metapneumovirus fusion: essential residues and importance in entry. J. Virol. **83**:1511–1522.
58. **Simon M, Johansson C, Mirazimi A.** 2009. Crimean-Congo hemorrhagic fever virus entry and replication is clathrin-, pH- and cholesterol-dependent. J. Gen. Virol. **90**:210–215.
59. **Stiasny K, Allison SL, Marchler-Bauer A, Kunz C, Heinz FX.** 1996. Structural requirements for low-pH-induced rearrangements in the envelope glycoprotein of tick-borne encephalitis virus. J. Virol. **70**:8142–8147.
60. **Struthers JK, Swanepoel R, Shepherd SP.** 1984. Protein synthesis in Rift Valley fever virus-infected cells. Virology **134**:118–124.
61. **Thoennes S, et al.** 2008. Analysis of residues near the fusion peptide in the influenza hemagglutinin structure for roles in triggering membrane fusion. Virology **370**:403–414.
62. **Tischler ND, Gonzalez A, Perez-Acle T, Rosemblatt M, Valenzuela PD.** 2005. Hantavirus Gc glycoprotein: evidence for a class II fusion protein. J. Gen. Virol. **86**:2937–2947.
63. **Vaney MC, Rey FA.** 2011. Class II enveloped viruses. Cell. Microbiol. **13**:1451–1459.
64. **Wahlberg JM, Garoff H.** 1992. Membrane fusion process of Semliki Forest virus. I. Low pH-induced rearrangement in spike protein quaternary structure precedes virus penetration into cells. J. Cell Biol. **116**:339–348.
65. **Walter CT, Barr JN.** 2011. Recent advances in the molecular and cellular biology of bunyaviruses. J. Gen. Virol. **92**:2467–2484.
66. **Wang GJ, Hewlett M, Chiu W.** 1991. Structural variation of La Crosse virions under different chemical and physical conditions. Virology **184**:455–459.
67. **Weissenhorn W, Hinz A, Gaudin Y.** 2007. Virus membrane fusion. FEBS Lett. **581**:2150–2155.
68. **White J, Matlin K, Helenius A.** 1981. Cell fusion by Semliki Forest, influenza, and vesicular stomatitis viruses. J. Cell Biol. **89**:674–679.
69. **Yoshimura A, et al.** 1982. Infectious cell entry mechanism of influenza virus. J. Virol. **43**:284–293.